Bioorganic & Medicinal Chemistry 20 (2012) 1388–1395

Contents lists available at SciVerse ScienceDirect

Bioorganic & Medicinal Chemistry

journal homepage: www.elsevier.com/locate/bmc

QSAR study and synthesis of new phenyltropanes as ligands of the dopamine transporter (DAT)

Sylvie Mavel [a,b,*], Zoya Mincheva [a], Nathalie Méheux [a], Yvan Carcenac [c], Denis Guilloteau [a,b], Mohamed Abarbri [c], Patrick Emond [a,b]

[a] Université François-Rabelais, INSERM U930, CNRS ERL3106, 31 Avenue Monge, 37200 Tours, France
[b] INSERM U930, CHRU, Hôpital Bretonneau, 37000 Tours, France
[c] Université François-Rabelais, Laboratoire de Physicochimie des Matériaux et Biomolécules EA 4244, Faculté des Sciences, 37200 Tours, France

ARTICLE INFO

Article history:
Received 3 November 2011
Revised 4 January 2012
Accepted 9 January 2012
Available online 18 January 2012

Keywords:
Dopamine transporter
Iodine
3D-QSAR
Tropane

ABSTRACT

The dopamine transporter (DAT) plays a pivotal role in the regulation of dopamine neurotransmission, and is involved in a number of physiological functions and brain disorders. Furthermore the DAT analysis by molecular imaging techniques is a useful tool for the diagnosis and follow up treatment of diseases involving the DAT. In order to predict the affinity of new derivatives for the DAT, different QSAR molecular modeling models based on cocaine were compared. We have evaluated in these models tropane derivatives synthesized with original synthons which coupled properties of both fluorine and iodine atoms. One compound showed a high in vitro affinity and selectivity for the DAT (K_i = 0.87 ± 0.04 nM). This compound should be radiolabeled with radioiodine for further investigations by SPECT.

1. Introduction

Dopamine (DA) is one of the key central nervous system (CNS) neurotransmitters involved in the mediation and/or control of a variety of physiological functions, including movement, emotion, and cognition.[1] DA, which does not cross the blood–brain barrier, is synthesized from tyrosine in presynaptic neurons and is subsequently concentrated in vesicles for a later release in the synaptic cleft.[2] The released DA binds to pre- and post-synaptic receptors, involved in a series of biological events. Two main processes regulate the concentration of DA in the synapse and thus the intensity and duration of dopaminergic neurotransmission. The first process involves monoamine oxidases and catecholamine *O*-methyl transferases, which metabolize DA, while the second involves the dopamine transporter (DAT), a presynaptic transmembrane protein that accumulates DA into presynaptic neurons.[3,4] The dopamine transporter has a crucial function and it has been shown to be involved in depression,[5] schizophrenia, Parkinson's disease (PD),[6,7] Attention Deficit Hyperactivity Disorder (ADHD),[8] and drug abuse (e.g., cocaine or methamphetamine).[9,10] Thus DAT has been extensively studied either by using in vitro methods or through in vivo imaging by Single-Photon Emission Computed Tomography (SPECT) and Positron Emission Tomography (PET). Because DAT serves as a selective marker of dopamine terminal innervations in the striatum, DAT-based imaging has been proposed as an early diagnostic test for PD[11] which is characterized by a selective loss of dopamine neurons in the basal ganglia and substantia nigra.[12–15]

Cocaine (Fig. 1) has been found to be an inhibitor of dopamine, but also serotonin (SERT) and norepinephrine (NET) transporters. It was also demonstrated that the replacement of the benzoyl group with a phenyl group attached directly to the 3β-position of the tropane skeleton (Fig. 1) led to derivatives with higher affinities for the DAT than cocaine itself.[9] Several attempts have been made to radiolabel and structurally modify the β-phenyltropane skeleton on either the *N*-methyl, the *O*-methyl ester or the phenyl group to increase the selectivity of tropane structure for the DAT.[16–24]

Many radiolabeled 3β-phenyltropane derivatives,[25] which can specifically bind to DAT, have been prepared and studied for in vivo imaging of DAT with PET or SPECT. The first compound used successfully in vivo was β-CIT (Fig. 1). The decrease in specific DAT binding of ^{123}I-β-CIT in SPECT studies was found to be correlated with the progression of PD symptoms.[26]

In light of these studies, our efforts focused on the design and synthesis of iodinated cocaine derivatives,[27] in particular at the bridgehead nitrogen and at the 4-position of the phenyl ring, which exhibited high affinity and specificity for the DAT.[28] Among the series of compounds synthesized, *N*-(3-iodoprop-2*E*-enyl)-2β-car-

Abbreviations: DAT, dopamine transporter; QSAR, quantitative structure–activity relationship; SPECT, Single Photon Emission Computed Tomography.

* Corresponding author. Address: Faculté de Pharmacie, Laboratoire de Biophysique Médicale et Pharmaceutique, 31 Avenue Monge, 37200 Tours, France. Tel.: +33 2 47 36 72 40; fax: +33 2 47 36 72 24.
E-mail address: sylvie.mavel@univ-tours.fr (S. Mavel).

0968-0896/$ - see front matter © 2012 Elsevier Ltd. All rights reserved.
doi:10.1016/j.bmc.2012.01.014

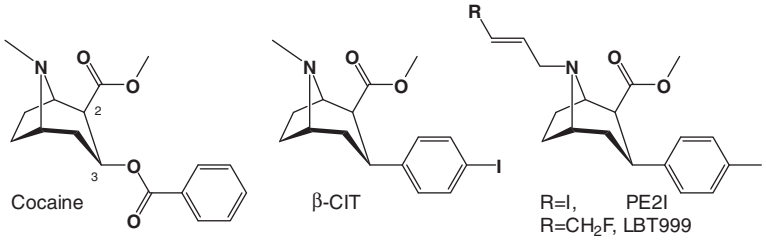

Figure 1. Cocaine and analogs.

bomethoxy-3β-(4-methylphenyl)nortropane (PE2I, Fig. 1) was selected as a very potent radiopharmaceutical to image the DAT in vivo by PET and SPECT.[29,30] But, even if tropane derivatives have good and selective in vitro affinities, too often, poor bioavailability or slow pharmacokinetics contributes to altering their in vivo action, making the development of DAT ligand a great challenge.

To rationalize the variations observed in binding affinities for the DAT, structure–activity relationship (SAR) studies for different classes of DA reuptake inhibitors have been done.[31,32] To expand these efforts, we report here different 3D quantitative structure activity relationships (QSAR), based on 69 tropane derivatives and analogs (Fig. 2, and Supplementary data).

Aiming to improve the pharmacokinetics of DAT ligands, we have taken into account the fact that the introduction of a fluorine or perfluoroalkyl group into organic compounds might dramatically change their structure, stability, reactivity and biological activity.[33,34] We present here the design and the synthesis of new tropane derivatives bearing synthons which, to our knowledge, have never been biologically evaluated. Theses groups (trifluoro-iodo-butene) possess both an iodine atom for radiolabeling and fluorine which could improve the potency and/or the pharmacokinetics properties of the drug. QSAR models have been used to predict the binding affinity of these original tropanes **4** and **5**. These two compounds have been synthesized, and then evaluated in vitro against monoamine transporters.

2. Results and discussion

2.1. Molecular modeling: QSAR studies

During the last decade, substantial structural information based on the tropane skeleton have been obtained by QSAR studies, and thus different pharmacophore models have already been proposed.[31,35–39] In general, a basic substituted nitrogen on the tropane ring in a *R*-configuration, along with a hydrogen bond acceptor corresponding to the two oxygen atoms for the ester group, and a phenyl group seems to be the most cited pharmacophores.[25]

The transporter binding potency could be reported as IC_{50} and this IC_{50} value could be converted to an absolute inhibition constant K_i as the uptake inhibition value. As IC_{50} values change with experimental conditions, we focused on literature data given K_i values (for more details, see Supplementary data). For calculation, $pK_i = -\log K_i$ was used. DAT binding K_i's range from 0.4 nM to 2400 nM, so with a spread of values which exceeded 3.5 orders of magnitude as suggested for QSAR studies (all derivatives varied in DAT affinities over about 3.3 log units).

The QSAR studies described here are based on 69 derivatives belonging to the tropane skeleton classes (I–IV) and other bicyclic structures (V–VI) (Fig. 2, Supplementary data). The QSAR software (Discovery Studio® 2.5, Accelrys, Inc., San Diego, CA) present 179 physicochemical descriptors: electronic, spatial, shadow, shape and thermodynamic indices. After several filters (analyzing the correlation matrix, eliminating the highly correlated descriptors), and eliminating descriptors with too wide a range of training data (>700), only 27 2D or 3D descriptors were retained as dependent on K_i. The definitions of main descriptors obtained in QSAR studies are given in Table 2, their correlation is given in Supplementary data.

We compared three different QSAR methods (Table 1): the Multiple Linear Regression (MLR), the Partial Least Squares (PLS), and the Genetic Function Approximation (GFA) algorithms.[40] In the GFA model, we chose linear terms of descriptors as in a previous paper where quadratic terms were unsatisfactory for predictive determinations.[41] For the statistical parameters, *R*-squared r^2 is chosen (Table 1) and for GFA model, the standard errors of regres-

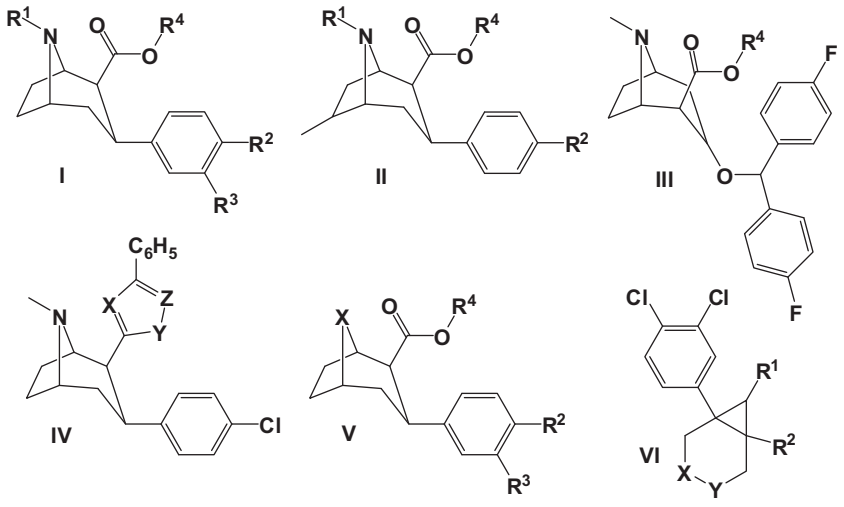

Figure 2. General structures of DAT ligands used for QSAR studies.

Table 1
Statistics from the regression modeling procedure (69 samples)

Model	r^2	r^2 (adj)	r^2 (pred)		Friedman L.O.F.	$pK_{i-predictif}$ for **4**	$pK_{i-predictif}$ for **5**
MLR	0.814	0.692	0.150	Least-squared Error = 0.1369	—	6.86	8.10
PLS	0.807	0.732	—	Least-squared Error = 0.1424	—	7.48	8.99
GFA	0.718	0.670	0.560	RMS residual Error = 0.4966	1.105	6.80	7.63

Predictive binding affinity (pK_i) for the two original compounds **4** and **5**.

Table 2
Description of the molecular properties used as descriptors in QSAR studies

Descriptor	Description	Order of priority in the model
log*D*[a]	Octanol/water partition coefficient	
ES_Count_dsCH[b]	Count of electrotopological state values for CH atoms	
ES_Count_dssC[b]	Count of electrotopological state values for C atoms	
ES_Count_sI[b]	Count of electrotopological state values for I atoms	
ES_Sum_sCH3[b]	Sums of electrotopological state values for CH_3 atoms	6th—GFA
Num_H_Acceptors[c]	Hydrogen bond acceptors are defined as heteroatoms with one or more lone pairs	5th—MLR 3rd—PLS 2nd—GFA
Num_H_Donors[c]	Hydrogen bond donors are defined as heteroatoms with one or more hydrogen atoms	5th—GFA
BIC[d]	Graph-theoretical info content descriptor which differentiate molecules according to their size, degree of branching, and flexibility. Bonding information content	2nd—MLR 1st—GFA
CHI-V_3_P[d]	Kier and Hall valence-modified connectivity index amount of branching, ring structures present, and flexibility	6th—MLR 4th—PLS 3rd—GFA
IAC_Mean[d]	Graph-theoretical info content descriptor: mean information of atomic composition	3rd—MLR 5th—PLS
JX[d]	Highly discriminating descriptor. This Balaban indice characterize the shape of a molecule taking into account electronegativity of the atoms of the model	4th—MLR 2nd—PLS
Shadow YZ frac[e]	Projection of molecular surface on a plan (YZ)	6th—PLS
Dipole Z[f]	Dipole moment	
Jurs_FPSA_3[g]	Map of atomic partial charges on solvent-accessible surface areas of individual atoms: fractional partial positive solvent accessible surface areas	
Jurs_PPSA_1[g]	Atomic charge weighted positive surface area	
Molecul_Volume[g]	Molecular_Volume	1st—MLR 1st—PLS 4th—GFA

Order of priority of the six first major contributing factors.
[a] Thermodynamic descriptor.
[b] Estate keys.
[c] Molecular property counts.
[d] 2D topological descriptor.
[e] Spatial, 3D descriptor.
[f] 3D electronic descriptor.
[g] 3D descriptor.

sion coefficients are given in parentheses. The Friedman's lack-of-fit (LOF) score which evaluates the QSAR model with GFA algorithm by considering the number of descriptors as well as the quality of fitness is given as well. The lower the LOF, the less likely it is that the GFA model will fit the data.

We have designed new structures bearing a trifluoro-iodobutene group to predict the biological impact of this new synthon. The validated model was then used to predict the binding affinity for these two new structures **4** and **5**.

Set 1: MLR model

$pK_{i-pred} = -5.02 + 0.7056 * \log D + 1.25414 * Num\_H\_Acceptors + 10.9567 * BIC + 3.41408 * CHI\_V\_3\_C + 5.75802 * IAC\_Mean - 3.4142 * JX - 0.30163 * Dipole\_Z - 57.92 * Jurs\_FPSA\_3 + 3.64297 * Shadow\_YZfrac - 0.04695 * Molecular\_Volume.$

Set 2: PLS model

$pK_{i-pred} = 10.4467 - 1.08175 * ES\_Count\_dssC + 0.63107 * \log D + 1.8233 * Num\_H\_Acceptors - 0.72543 * Num\_H\_Donors + 4.32905 * CHI\_V\_3\_C + 2.50941 * IAC\_Mean - 3.32627 * JX - 0.00405 * Jurs\_PPSA\_1 + 3.07894 * Shadow\_YZfrac - 0.04778 * Molecular\_Volume.$

Set 3: GFA model

$pK_{i-pred} = 0.75\ (\pm 2.08) + 0.53267\ (\pm 0.10) * ES\_Count\_dsCH - 1.0933\ (\pm 0.31) * ES\_Count\_dssC - 1.1082\ (\pm 0.19) * ES\_Count\_sI - 0.36448\ (\pm 0.04) * ES\_Sum\_sCH3 + 1.2153\ (\pm 0.22) * Num\_H\_Acceptors - 0.85877\ (\pm 0.19) * Num\_H\_Donors + 5.9432\ (\pm 2.00) * BIC + 3.488\ (\pm 0.58) * CHI\_V\_3\_C - 0.15951\ (\pm 0.08) * Dipole\_Z - 0.01126\ (\pm 0.004) * Molecular\_Volume.$

The three models (MLR, PLS, and GFA) gave good *R*-squared r^2 values (0.81, 0.81 and 0.72, respectively). These three methods showed a difference in predictive affinity for the DAT between **4** and **5**: they all predicted a better affinity for **5** for the DAT, and the best predictive value for **5** was obtained with the MLR model (Table 2). From 27 descriptors, the QSAR models developed there revealed three common descriptors and proved the importance of simple molecular characteristics essential for DAT affinity. These include the 'Molecular_Volume', a 3D descriptor. For derivative **5**, the iodine atom is close to the tropane skeleton, this compound

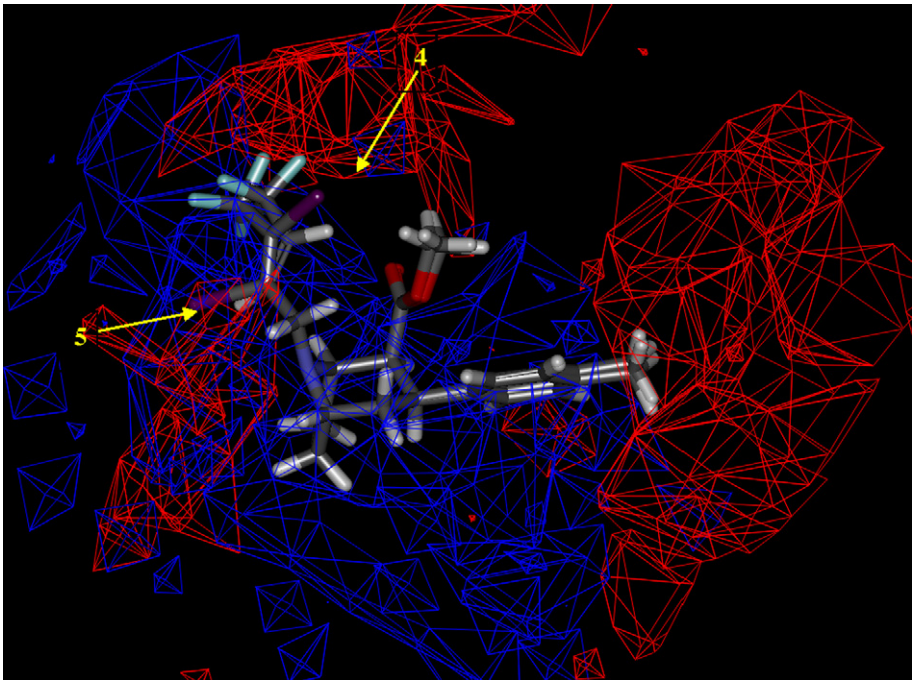

Figure 3. Isosurface of the 3D-QSAR model coefficients on electrostatic potential grids with positive electrostatic potential in red triangle mesh representation and the negative in blue area for the aligned molecular structures of 68 ligands. Derivatives **4** and **5** are shown in stick representation while the iodine atoms are designed by the arrows.

presents a smaller value than its isomer (Molecular_Volume $_{(5)}$ = 274.7 compared to Molecular_Volume $_{(4)}$ = 281.9) and since this descriptor is unfavorable for the affinity, the more compact the structure, the better the affinity.

One major descriptor for MLR and GFA models is a 'graph-theoretical info-content' 2D descriptor: BIC, which differentiate molecules according to their size, degree of branching, and flexibility. Molecules are viewed as structures that can be partitioned into subsets of elements that are in some sense equivalent. The mean value for BIC calculations for the 69 compounds is 0.789. As the coefficient in the equation is positive, the bigger the value, the better the affinity for the DAT (BIC $_{(5)}$ = 0.763 compared to BIC $_{(4)}$ = 0.748).

An other positive descriptor for MLR and PLS model is a 'graph-theoretical info-content' descriptor: 'IAC_mean' which corresponds to the main information of the atomic composition. The mean value for the 69 compounds is 1.492, **4** and **5** have the same value of 1.699 which favors their affinity compared to the majority of DAT ligands according to 'IAC_mean' descriptor.

The JX (a Balaban index which characterizes the shape of a molecule taking into account the relative covalent radius of the atoms of the model) is also an important descriptor for MLR and PLS

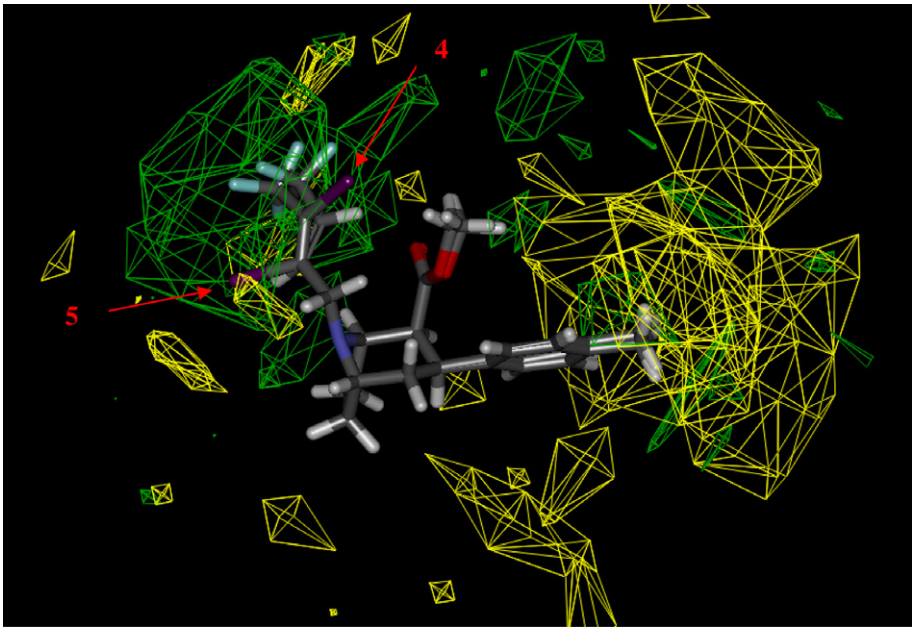

Figure 4. Isosurface of the 3D-QSAR model coefficients on Van der Waals grids. The green triangle mesh representation indicates positive coefficients; the yellow triangle mesh indicates negative coefficients. Derivatives **4** and **5** are shown in stick representation while the iodine atoms are designed by the arrows.

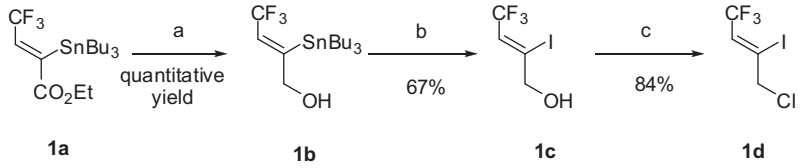

Scheme 1. Preparation of (*Z*)-4-chloro-1,1,1-trifluoro-3-iodobut-2-ene **1d**. Reagent and conditions: (a) DIBAL-H, THF, −60 °C; (b) I_2, CH_2Cl_2, 0 °C; (c) $SOCl_2$, pyridine, reflux.

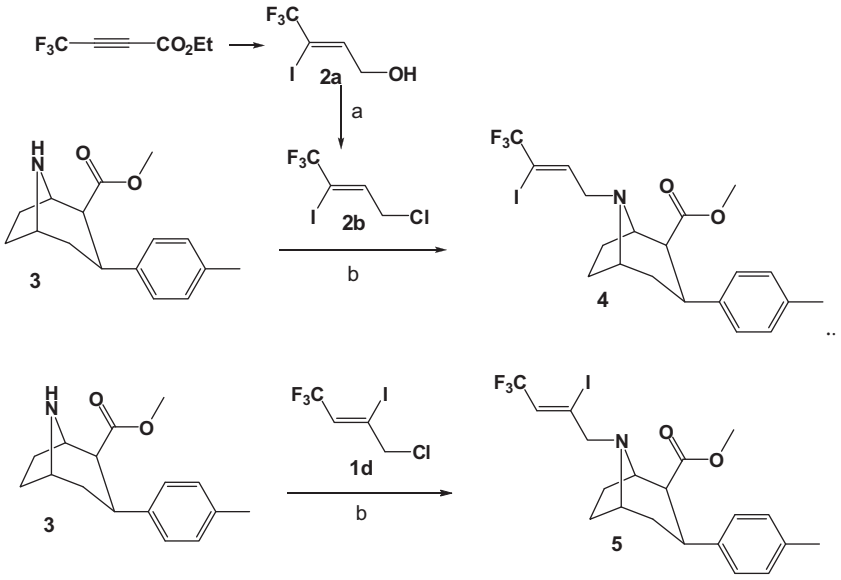

Scheme 2. Preparation of **4** and **5**. Reagent and conditions: (a) $SOCl_2$, pyridine, reflux; (b) EtOH, Et_3N, KI, reflux.

models. As the coefficient in the equation is negative, the smaller the value, the better the affinity for the DAT. For both compounds **5** and **4**, their JX value was close to the mean value for the 69 compounds given to 1.81 (JX_{5} = 1.8122 and JX_{4} = 1.8022).

Finally the topological descriptor present in the three models concerns the connectivity indices: CHI_V_3_C. Its calculation is derived from the 2D topology of the molecule. The mean value for the 69 compounds is 1.045, for derivative **5** this favorable descriptor is bigger than for derivative **4** ($CHI\_V\_3\_C_{(5)}$ = 1.533 compared to $CHI\_V\_3\_C_{(4)}$ = 1.365).

MLR, PLS, and GFA models were tested with **4** and **5**, with the predictive subnanomolar K_i (Table 1) for **5**, furthermore, these models found a difference with its isomer **4**.

The 3D-QSAR model (Discovery Studio® 2.5, Accelrys), defines the critical regions (steric or electrostatic) affecting the binding affinity. It was a PLS model built on 400 independent variables (N = 68, r = 0.893 and r^2 = 0.763). A contour plot of the electrostatic field region favorable (in blue) or unfavorable (red) for the DAT affinity is shown in Figure 3 with the superposition of both isomers **4** and **5**. The energy grids corresponding to the favorable (in green) or unfavorable (yellow) steric effects for the DAT affinity are shown in Figure 4 with the superposition of both isomers **4** and **5**. A good ligand should have strong Van der Waals attraction in the green areas and a polar group in the blue electrostatic potential areas (which are dominant close to the skeleton). Several key features of the 3D-QSAR contour map are predicted to increase DAT affinity:

- Less bulk near the *para* position on the phenyl group (steric study).
- More bulk group substituted on the nitrogen, at a distance of more than 5 Å from the nitrogen (steric study).
- A more positive environment all around the *para* position of the phenyl ring (electronic study).
- A more negative environment around the nitrogen, but with well delineated zones for positive group (electronic study).

From this 3D model, binding affinity of both isomers **4** and **5** was predicted: pK_i = 7.95 and 8.24, respectively.

From these four QSAR studies, **5** was predicted to possess nanomolar affinity for DAT in all cases, with significant differences with its isomer **4** which is predicted to exhibit less affinity.

2.2. Chemistry

The development of a simple method to obtain perfluoroalkylated building blocks for their subsequent utilization in medicinal chemistry for R_F-containing compounds is essential to organofluorine chemistry.[42–46] As a continuation of previous methods of preparing various derivatives bearing a trifluoromethyl group,[47] we have described the regio- and stereoselective synthesis of (*Z*)-α-tributylstannyl-β-trifluoromethylacrylate[48] using a simple free-metal hydrostannylation of ethyl-4,4,4-trifluorobut-2-ynoate. We report here the highly regioselective synthesis of (*Z*)-4-chloro-1,1,1-trifluoro-3-iodobut-2-ene **1d** starting from (*Z*)-ethyl-2-tributylstannyl-3-trifluoromethyl but-2-enoate **1a** (Scheme 1).

Reduction of ester **1a** with DIBAL-H in THF provided quantitatively the desired alcohol **1b** with retention in the configuration. The *Z* stereochemistry of **1b** was assigned taking into account that the $^3J_{Sn-H}$ coupling constant observed in the ^1H NMR spectra was over 70 Hz, which indicates the existence of *trans* H-C-C-Sn linkages in these compounds.[49–51] Iododestannylation of the vinylstannanes with iodine gave the corresponding 2-iodo-3-trifluoromethyl allylic

Table 3
Binding affinities of the new derivatives **4** and **5** for monoamine transporters, lipophilicity measurements and predictions for **4**, **5** and references derivatives (PE2I and LBT999[53]).

Compd	hDAT [^{3}H]WIN35428 K_i[a] (nM)	hSERT [^{3}H]Citalopram K_i[a] (nM)	hNET [^{3}H]Nisoxetine K_i[a] (nM)	(HPLC) log$P_{7.4}$ [e]	Discovery Studio, Accelrys® *A*log*P*	Chem Draw® *c*log*P*[f]
PE2I	17 ± 7[b]	>1000[b]	>500[b]	4.9	3.66	4.71
LBT999	9[c]	>1000[d]	>1000[d]	4.1	3.94	3.53
4	116 ± 8.5	251 ± 6.6	426 ± 18.7	5.3	4.83	4.98
5	0.87 ± 0.04	>1000	188 ± 23	5.5	4.83	4.98

[a] Inhibition constants (K_i) were obtained from the mean ± SD of four separate determinations each in triplicate.
[b] Inhibition constants (K_i) are given in literature.[28]
[c] K_d (nM) value is given in literature.[54]
[d] IC_{50} (nM) are given in literature.[54]
[e] Reverse-phase HPLC experiments.
[f] Calculated *c*log*P* (ChemDraw Ultra 10.0, 2005, CambridgeSoft Corporation, USA).

alcohol **1c** with no change of the configuration of the double bond. The compound **1c** was subsequently converted to the corresponding (*Z*)-1-chloro-2-iodo-4,4,4-tifluorobut-2-ene **1d** using $SOCl_2$ in dry pyridine at 0 °C for 12 h to provide the desired chloride **1d** in 84% yield. The (*Z*)-olefinic configuration of **1d** was confirmed by the strong NOE correlation between the vinylic proton and the allylic protons in the NOESY spectrum of **1d**. (*Z*)-1-chloro-3-iodo-4,4,4-tifluorobut-2-ene **2b** (Scheme 2) was obtained in good yield (78%) from **2a**[48] using the same conditions described above for compound **1d**.

Derivatives **4** and **5** were prepared from cocaine, via the intermediate tropanamine **3**,[28] namely 3β-*p*-tolyl-8-aza-bicyclo[3.2.1] octane-2β-carboxylic acid methyl ester (Scheme 2). Condensation of **3** with **1d** or **2b** in ethanol with triethylamine at reflux for 6 h gave derivatives **4** or **5** in 59% or 75% yield, respectively (Scheme 2).

Furthermore, we studied by molecular modeling energy calculation (DiscoveryStudio® 2.5, Accelrys) the potential stability of these trifluoro-iodo-butene skeletons. Compound **5** with a 4-trifluoro-2-iodo but-2-ene group was found to be more stable than its isomer **4** (E(**5**) = 33.126 kcal/mol compared to E(**4**) = 40.110 kcal/mol), and so, potentially more stable in vivo, especially for the C–I bond since E(C–I) for compound **5** was found to be 0.007484 kcal/mol compared to 0.016986 kcal/mol for compound **4**.

2.3. In vitro affinity, selectivity and lipophilicity

The in vitro affinities of **4** and **5** were evaluated by competition studies using tritiated ligands of SERT ([^{3}H]citalopram), DAT ([^{3}H]GBR12935), and NET ([^{3}H]nisoxetine) (Table 3). For each compound and each transporter, K_i values were determined when 100 nM of a target compound inhibited at least 50% of tritiated ligand binding (IC_{50} <100 nM) in accordance with the previously published procedure.[52]

In vitro binding experiments showed that **4** bound with low affinities to monoamine transporters. At the opposite, **5** exhibited high potency for the DAT (K_i = 0.87 nM) and selectivity over both hNET (216-fold) and hSERT (over 10,000-fold). The position of iodine seems critical to the affinity for the DAT. Compound **5** exhibited a better affinity for the DAT than LBT999 (Fig. 1) and PE2I (10- and 20-fold higher, respectively), two of the best ligands used at the moment to image the DAT in vivo. Therefore **5** is an attractive candidate as a SPECT radiotracer for imaging the DAT in the brain.

MLR, PLS, and GFA models were tested with **4** and **5**, giving the predictive subnanomolar K_i (Table 1) for **5** and these models found a difference with its isomer **4** as the experimental findings reported in Table 3 (pK_i = 9.06 and 6.93, respectively). From the 3D-QSAR model, binding affinity of both isomers **4** and **5** were predicted: pK_i = 7.95 and 8.24, respectively. This model could predict differences between the two derivatives but not as significant as the experimental findings.

Concerning the lipophilicity, in QSAR studies, log*D* [logarithm distribution cœfficient at pH 7 is used if ionizated molecular species are present: $\log D = \log P + \log 1/(1 + 10^{pka\text{-}pH})$, also referred to pH-dependant lipophilicity descriptor] was one of the main descriptor in MLR and PLS models, hence we focused on the lipophilicity of compounds **4** and **5**. For the QSAR studies, DiscoveryStudio algorithms were based on a fragmental method, as for *c*log*P* (ChemDraw®) (Table 3), and so the log*D* predictions could not be accurate in all cases. For compounds **4** and **5**, their unusual nitrogen substituent, for which the fragmental values are not in the list provided by the software library, the models were not able to predict accurately the lipophilicity and could not differentiate these two regio-isomers. We have alternatively measured log$P_{7.4}$ using a reverse-phase HPLC method for **4** and **5** (see Table 3). In the MLR and PLS models, as log*D* is favourable for the affinity, the smaller the value, the lower the affinity for the DAT. The experimental values of log$P_{7.4}$ given in Table 3 followed the same trend as the predicted models ($\log P_{7.4\ (4)} = 5.3$ compared to $\log P_{7.4\ (5)} = 5.5$). It is well recognized that drugs should have an optimum log$P_{7.4}$ around 3.0 to get a good balance between brain entrance and non specific binding, and even if compound **5** showed a high log*P*, it has a similar lipophilicity to some phenothiazines,[55] for example, used as antipsychotic. Therefore, **5** should be soon in vivo evaluated.

3. Conclusions

We obtained good linear MLR and PLS QSAR models and a 3D-QSAR model, which confirmed the spatial impact on affinity for DAT via steric descriptors and the Van der Waals coefficient. Two new tropane analogs bearing a trifluoro-iodobutene group, which seems to be a stable and promising synthon, were synthesized and tested as dopamine transporter ligands for potential use as SPECT imaging agents. The 3-iodo-4-trifluorobutene-tropane showed good in vitro potency for the DAT as predicted by each QSAR study which calculated a better affinity for **5** compared to the less stable *gem*-disubstituted derivative **4**.

Derivative 5 will soon be evaluated in vivo as potential SPECT imaging agent for mapping DAT in rodent brain.

4. Experimental section

4.1. Molecular modeling

Computational results were obtained using software programs from Accelrys Software Inc. The molecules were built and minimized in molecular package (Discovery Studio® 2.5.5, Accelrys, San Diego, CA) by CHARMm with CFF partial charge estimation method. The 3D structures were generated and optimized using a CHARMm forcefield with a root mean squared (RMS) difference of energy gradient of 0.1 kcal/mol. The GFA model in QSAR protocol

was used with a population size of 100 and 5000 maximum generations. All the parameters have been left to the system defaults. Two model forms have been used: linear or full quadratic. For the 3D-QSAR model, the grid spacing was 1 Å.

4.2. Chemistry

NMR spectra were recorded on a Bruker DPX Avance 200 spectrometer (200 MHz for ^{1}H, 50.3 MHz for ^{13}C). $CDCl_3$ was used as solvent; chemical shifts are expressed in ppm relative to TMS as an internal standard. IR spectra were obtained on an Alpha-E FT-IR spectrometer (Bruker) with ATR crystal. Mass spectra were obtained on a CG–MS Hewlett Packard 5989A spectrometer (electronic impact at 70 eV). Fragmentation of tropane derivatives was in accordance with previous work.[56] The thin-layer chromatographic (TLC) analyses were performed using Merck 60-F_{254} silica gel plates. Flash chromatography was used for routine purification of reaction products using silica gel (230–400 Mesh). Visualization was accomplished using UV or on an iodine chamber. All chemicals and solvents are commercial available and were purified following standard procedures.

Compounds **1a**,[48] **2a**[57] and 3β-*p*-tolyl-8-aza-bicyclo[3.2.1]octane-2β-carboxylic acid methyl ester **3**[28] were synthesized as previously described. The spectral data of **1c** have been previously reported in the literature.[58]

4.2.1. (*Z*)-4,4,4-Trifluoro-2-(tributylstannyl)but-2-en-1-ol (1b)

A solution of DIBAL-H (1 M in hexane, 7.2 mL, 7.2 mmol) was added dropwise at −60 °C to a solution of (*Z*)-ethyl 4,4,4-trifluoro-2-(tributylstannyl)but-2-enoate (**1a**, 1.37 g, 3.00 mmol) in THF (25 mL). The mixture was stirred for 30 min at −60 °C, and then for 4 h at room temperature. A saturated solution of NH_4Cl (20 mL) was added and the aqueous layer was extracted with diethylether (3 × 20 mL). The ether layers were combined, washed with brine (50 mL), dried over anhydrous $MgSO_4$ and filtered. The solvent was evaporated under vacuum. The crude product (1.24 g, 3.00 mmol, quantitative yield) was used without further purification in the following reaction step: ^{1}H NMR (200 MHz, $CDCl_3$): δ 0.85–1.60 (m, 28H), 4,38 (m, 2H), 6.51 (qt, 1H, $^3J_{H\text{-}F}$ = 7.7 Hz, $^4J_{H\text{-}H}$ = 2.2 Hz, $^3J_{Sn\text{-}H}$ = 75 Hz); ^{13}C NMR (50 MHz, $CDCl_3$): δ 10.3, 13.6, 27.3, 28.9, 67.9, 123.5 (q, ^2J = 33 Hz), 124.1 (q, ^1J = 270 Hz), 158.3 (q, ^3J = 6 Hz); MS: *m/z* (%): 359 (*M*−57, 56), 251 (100), 177 (48), 137 (41), 57 (48).

4.2.2. (*Z*)-4,4,4-Trifluoro-2-iodobut-2-en-1-ol (1c)

Iodine (1.36 g, 5.36 mmol) was added at 0 °C to a solution of (*Z*)-4,4,4-trifluoro-2-(tributylstannyl)but-2-en-1-ol (**1b**, 1.00 g, 2.41 mmol) in dichloromethane (25 mL). The mixture was stirred for 2 h at 0 °C and water (25 mL) was added, and the aqueous layer was extracted with dichloromethane (3 × 20 mL). The organic layers were combined, washed with aqueous $Na_2S_2O_3$ (50 mL) and brine (50 mL), dried over anhydrous $MgSO_4$ and filtered. After removal of the solvent under vacuum, the residue was purified by flash chromatography on silica gel (petroleum ether/Et_2O: 8/2) to afford **1c** (0.41 g, 67%) as a brown oil.

4.2.3. (*Z*)-4-Chloro-1,1,1-trifluoro-3-iodobut-2-ene (1d)

Thionyl chloride (0.16 mL, 2.19 mmol) was added dropwise to a solution of (*Z*)-4,4,4-trifluoro-2-iodobut-2-en-1-ol (**1c**, 0.50 g, 1.98 mmol) in pyridine (0.16 mL, 1.98 mmol). The mixture was stirred at room temperature for 15 min, refluxed for 30 min, and allowed to cool to room temperature. Diethyl ether was added (10 mL) and the organic phase was washed successively with water (10 mL), aqueous sodium bicarbonate (10 mL) and brine (10 mL), dried over anhydrous $MgSO_4$ and filtered. The solvent was removed under vacuum to give the crude **1d** as a brown oil (450 mg, 84%): ^{1}H NMR (200 MHz, $CDCl_3$): δ 4.42 (t, 2H, $^4J_{H\text{-}H}$ = 2.0 Hz), 6.82 (qt, $^3J_{H\text{-}F}$ = 7.0 Hz, $^4J_{H\text{-}H}$ = 2.0 Hz); ^{13}C NMR (50 MHz, $CDCl_3$): δ 52.7, 106.0 (q, ^3J = 6 Hz), 121.3 (q, ^1J = 270 Hz), 127.1 (q, ^2J = 36 Hz); MS: *m/z* (%): 270 (*M*+, 44), 143 (100), 108 (52), 93 (17), 57 (39).

4.2.4. (*Z*)-4,4,4-Trifluoro-3-iodobut-2-en-1-ol (2a)

^{1}H NMR (200 MHz, $CDCl_3$): δ 3.44 (br s, 1H), 4.27 (d, $^3J_{H\text{-}H}$ = 5.1 Hz, 2H), 6.86 (tq, $^3J_{H\text{-}H}$ = 5.1 Hz, $^4J_{H\text{-}F}$ = 1.3 Hz, 1H); ^{13}C NMR (50 MHz, $CDCl_3$): δ 65.8, 87.0 (q, ^2J = 37 Hz), 120.2 (q, ^1J = 271 Hz), 143.9 (q, ^3J = 5 Hz); MS: *m/z* (%): 252 (*M*+, 11), 232 (34), 105 (100), 77 (87).

4.2.5. (*Z*)-4-Chloro-1,1,1-trifluoro-2-iodobut-2-ene (2b)

Compound **2b** was prepared from derivative **2a** (0.50 g, 1.98 mmol) using the procedure described above for **1d**. Compound **2b** was purified by flash chromatography (EtOAc/petroleum ether: 1/9) to yield **2b** as a white solid (0.42 g, 78%): ^{1}H NMR (200 MHz, $CDCl_3$): δ 4.17 (dq, $^3J_{H\text{-}H}$ = 6.9 Hz, $^5J_{H\text{-}F}$ = 1.7 Hz, 2H), 6.81 (tq, $^3J_{H\text{-}H}$ = 6.9 Hz, $^4J_{H\text{-}F}$ = 1.3 Hz, 1H); ^{13}C NMR (50 MHz, $CDCl_3$): δ 44.8 92.1 (q, ^2J = 37 Hz), 120.3 (q, ^1J = 272 Hz), 139.8 (q, ^3J = 6 Hz); MS: *m/z* (%): 270 (*M*+, 35), 143 (100), 108 (45), 93 (23), 57 (32).

4.2.6. (*Z*)-Methyl 3-*p*-tolyl-8-(4,4,4-trifluoro-3-iodobut-2-enyl)-8-aza-bicyclo[3.2.1]octane-2β-carboxylic acid methyl ester (4)

To a solution of 3β-*p*-tolyl-8-aza-bicyclo[3.2.1]octane-2β-carboxylic acid methyl ester (**3**, 87 mg, 0.33 mmol) in ethanol (6 mL) and Et_3N (50 μL) was added a solution of (*Z*)-4-chloro-1,1,1-trifluoro-2-iodobut-2-ene **2b** (81 mg, 0.30 mmol) dissolved in ethanol (2 mL). A catalytic amount of KI was added. The mixture was stirred at reflux for 6 h, and stirred overnight at room temperature. The solvent was evaporated under vacuum, the crude product was purified by flash chromatography (EtOAc/petroleum ether: 5/95 to 10/90) to yield **4** as a white solid (84 mg, 59%): ^{1}H NMR (200 MHz, $CDCl_3$): δ 1.68–1.83 (m, 3H, H-4, H-6, H-7), 2.04–2.18 (m, 2H, H-6, H-7), 2.30 (s, 3H, CH_3), 2.61 (td, 1H, $^3J_{H\text{-}H}$ = $^2J_{H\text{-}H}$ = 12.4 Hz, $^3J_{H\text{-}H}$ = 2.6 Hz, H-3), 2.90–3.13 (m, 4H, H-2, H-3, CH_2), 3.43 (m, 1H, H-1), 3.52 (s, 3H, CH_3), 3.62 (m, 1H, H-5), 6.68 (t, $^3J_{H\text{-}H}$ = 6.9 Hz, 1H, CH=), 7.09 (d, $^3J_{H\text{-}H}$ = 8.0 Hz, 2Har), 7.16 (d, $^3J_{H\text{-}H}$ = 8.0 Hz, 2Har); ^{13}C NMR (50 MHz, $CDCl_3$): δ 20.9 (CH_3), 25.9, 26.4 (C-6, C-7), 33.5 (C-3), 34.0 (C-4), 50.9 (CH_3), 52.5 (C-2), 58.1 (NCH_2), 62.0 (C-5), 62.8 (C-1), 88.0 (q, ^2J = 38 Hz, CI), 120.4 (q, ^1J = 271 Hz, CF), 127.1 (2CHar), 128.6 (2CHar), 135.3 (Car), 139.5 (=CH), 143.7 (Car), 171.6 (CO); IR: $\tilde{\nu}$ (cm^{-1}) 2922, 1742, 1269, 1128, 813 cm^{-1}; MS: *m/z* (%): 493 (M^+, 56), 366 (76), 303 (100), 190 (76), 176 (45) 108 (37), 68 (25); HRMS *m/z* calcd for $C_{20}H_{23}F_3INO_2$ 493.0726, found 493.0728.

4.2.7. (*Z*)-Methyl 3-*p*-tolyl-8-(4,4,4-trifluoro-2-iodobut-2-enyl)-8-aza-bicyclo[3.2.1]octane-2β-carboxylic acid methyl ester (5)

Compound 5 was prepared from derivative **3** (87 mg, 0.33 mmol) and **1d** (81 mg, 0.30 mmol) using the procedure described above. Compound 5 was obtained as a white solid in 75% yield: ^{1}H NMR (200 MHz, $CDCl_3$): δ 1.71–1.87 (m, 3H, H-4, H-6, H-7), 2.06–2.12 (m, 2H, H-6, H-7), 2.34 (s, 3H, CH_3), 2.74 (td, 1H, $^3J_{H\text{-}H}$ = ^2J = 12.4 Hz, $^3J_{H\text{-}H}$ = 2.6 Hz, H-3), 2.97–3.10 (m, 4H, H-2, H-3, CH_2), 3.28 (m, 1H, H-1), 3.51 (s, 3H, CH_3), 3.65 (m, 1H, H-5), 7.04–7.30 (m, 5H, CH=, 4Har); ^{13}C NMR (50 MHz, $CDCl_3$): δ 21.1 (CH_3), 26.1, 26.8 (C-6, C-7), 33.4 (C-3), 33.9 (C-4), 51.1 (CH_3), 52.8 (C-2), 61.7 (C-5), 64.0 (C-1), 68.1 (NCH_2), 114.5 (CI), 122.8 (q, ^1J = 267 Hz, CF), 127.1 (2CHar), 128.7 (2CHar), 135.4 (Car), 127.1 (q, ^2J = 38 Hz, =CH), 139.2 (Car), 171.9 (CO); IR: $\tilde{\nu}$ (cm^{-1}) 2951, 1743, 1274, 1121, 813 cm^{-1}; MS: *m/z* (%): 493 (M^+, 1), 364 (35), 306 (45), 188 (54), 175 (100), 120 (27), 68 (14); HRMS *m/z* calcd for $C_{20}H_{23}F_3INO_2$ 493.0726, found 493.0727.

4.3. In vitro binding studies

Candidate compounds were assayed for their affinities to the monoamine transporters (SERT, NET and DAT) in competitive binding experiments in vitro using cloned human receptors (hSERT, hNET, and hDAT) expressed on HEK-293 cells and the radioligands [^{3}H]citalopram (SERT), [^{3}H]nisoxetine (NET), and [^{3}H]GBR12935 (DAT), in accordance with the published procedures.[52] For experimental details please refer to the PDSP web site http://pdsp.med.unc.edu/.

4.4. Lipophilicity measurements

An indirect determination of the octanol–water partition coefficients was used to obtain the $\log P_{7.4}$ by reverse-phase C-18 HPLC studies by comparison of their retention time (in triplicate) to that of 11 reference compounds (2-naphthol, 3-nitrophenol, aniline, benzamide, benzylchloride, bromobenzene, diphenyl, hexachlorobenzene, naphthalene, pyridine, and toluene) for a training set, and 3 (phenol, quinoline, and thymol) for a validation set with known $\log P$ values as previously reported.[59,60] A Water XBridge, 5 μm 4.6 mm × 150 mm analytical column was used with methanol/0.1 M phosphate buffer (pH 7.4) (50/50) at a flow rate of 0.9 ml/min. The 11 standards used to produce a calibration equation were dissolved in the mobile phase as for the validation set. With the same HPLC conditions the retention time for methanol was recorded as t_0. In order to offset the influence of the solvent on the appearance time of the measured peak, the appearance time of the methanol peak (t_0, 1.90 min) was used as a control. As an alternative representation of t_R, the parameter $\log K_w$ was defined as $\log K_w = \log[(t_R - t_0)/t_0]$. A calibration straight of $\log K_w$ versus $\log P_{7.4}$ was obtained with an experimental calibration equation ($y = 1.9818 \cdot \log K_w + 2.0536$) with a R-squared r^2 of 0.97.

Acknowledgements

We thank INSERM for financial support. We thank Thi-Huu Nguyen for her help. We thank the 'Département d'analyses chimiques et S.R.M. biologique et médicale' (Tours, France) for chemical analyses. We thank Nabyl Merbouh for providing language help. K_i determinations were generously provided by the National Institute of Mental Health's Psychoactive Drug Screening Program, Contract # NO1MH32004 (NIMH PDSP). The NIMH PDSP is directed by Bryan L. Roth MD, PhD at the University of North Carolina at Chapel Hill and Project Officer Jamie Driscol at NIMH, Bethesda MD, USA.

Supplementary data

Supplementary data (structures and affinities of DAT ligands used for the QSAR studies, QSAR data, . . .) associated with this article can be found, in the online version, at doi:10.1016/j.bmc.2012.01.014.

References and notes

1. Wise, R. A. *Nat. Rev. Neurosci.* **2004**, *5*, 483.
2. Velasco, M.; Luchsinger, A. *Am. J. Ther.* **1998**, *5*, 37.
3. Kebabian, J. W.; Calne, D. B. *Nature* **1979**, *277*, 93.
4. Lotharius, J.; Brundin, P. *Nat. Rev. Neurosci.* **2002**, *3*, 932.
5. Kapur, S.; Mann, J. J. *Biol. Psychiatry* **1992**, *32*, 1.
6. Dawson, T. M.; Dawson, V. L. *Science* **2003**, *302*, 819.
7. Niznik, H. B.; Fogel, E. F.; Fassos, F. F.; Seeman, P. *J. Neurochem.* **1991**, *56*, 192.
8. Mazei-Robison, M. S.; Couch, R. S.; Shelton, R. C.; Stein, M. A.; Blakely, R. D. *Neuropharmacology* **2005**, *49*, 724.
9. Carroll, F. I.; Lewin, A. H.; Boja, J. W.; Kuhar, M. J. *J. Med. Chem.* **1992**, *35*, 969.
10. Ritz, M. C.; Lamb, R. J.; Goldberg, S. R.; Kuhar, M. J. *Science* **1987**, *237*, 1219.
11. Brooks, D. *Biomark. Med.* **2010**, *4*, 651.
12. Cropley, V. L.; Fujita, M.; Innis, R. B.; Nathan, P. J. *Biol. Psychiatry* **2006**, *59*, 898.
13. Zhang, J.; Zhu, L.; Du, J.; Liu, B. *Neural Regen. Res.* **2007**, *2*, 18.
14. Felicio, A. C.; Shih, M. C.; Godeiro-Junior, C.; Andrade, L. A.; Bressan, R. A.; Ferraz, H. B. *Neurologist* **2009**, *15*, 6.
15. Varrone, A.; Halldin, C. *J. Nucl. Med.* **2010**, *51*, 1331.
16. Abi-Dargham, A.; Gandelman, M. S.; DeErausquin, G. A.; Zea-Ponce, Y.; Zoghbi, S. S.; Baldwin, R. M.; Laruelle, M.; Charney, D. S.; Hoffer, P. B.; Neumeyer, J. L.; Innis, R. B. *J. Nucl. Med.* **1996**, *37*, 1129.
17. Asenbaum, S.; Brucke, T.; Pirker, W.; Podreka, I.; Angelberger, P.; Wenger, S.; Wober, C.; Muller, C.; Deecke, L. *J. Nucl. Med.* **1997**, *38*, 1.
18. Clarke, R. L.; Daum, S. J.; Gambino, A. J.; Aceto, M. D.; Pearl, J.; Levitt, M.; Cumiskey, W. R.; Bogado, E. F. *J. Med. Chem.* **1973**, *16*, 1260.
19. Fang, P.; Wu, C. Y.; Liu, Z. G.; Wan, W. X.; Wang, T. S.; Chen, S. D.; Chen, Z. P.; Zhou, X. *Nucl. Med. Biol.* **2000**, *27*, 69.
20. Goodman, M. M.; Keil, R.; Shoup, T. M.; Eshima, D.; Eshima, L.; Kilts, C.; Votaw, J.; Camp, V. M.; Votaw, D.; Smith, E.; Kung, M. P.; Malveaux, E.; Watts, R.; Huerkamp, M.; Wu, D.; Garcia, E.; Hoffman, J. M. *J. Nucl. Med.* **1997**, *38*, 119.
21. Jurisson, S. S.; Lydon, J. D. *Chem. Rev.* **1999**, *99*, 2205.
22. Kung, M. P.; Essman, W. D.; Frederick, D.; Meegalla, S.; Goodman, M.; Mu, M.; Lucki, I.; Kung, H. F. *Synapse* **1995**, *20*, 316.
23. Kung, M. P.; Stevenson, D. A.; Plossl, K.; Meegalla, S. K.; Beckwith, A.; Essman, W. D.; Mu, M.; Lucki, I.; Kung, H. F. *Eur. J. Nucl. Med.* **1997**, *24*, 372.
24. Seibyl, J. P.; Marek, K.; Sheff, K.; Zoghbi, S.; Baldwin, R. M.; Charney, D. S.; van Dyck, C. H.; Innis, R. B. *J. Nucl. Med.* **1998**, *39*, 1500.
25. Singh, S. *Chem. Rev.* **2000**, *100*, 925.
26. Varrone, A.; Marek, K. L.; Jennings, D.; Innis, R. B.; Seibyl, J. P. *Mov. Disord.* **2001**, *16*, 1023.
27. Emond, P.; Helfenbein, J.; Chalon, S.; Garreau, L.; Vercouillie, J.; Frangin, Y.; Besnard, J. C.; Guilloteau, D. *Bioorg. Med. Chem.* **2001**, *9*, 1849.
28. Emond, P.; Garreau, L.; Chalon, S.; Boazi, M.; Caillet, M.; Bricard, J.; Frangin, Y.; Mauclaire, L.; Besnard, J. C.; Guilloteau, D. *J. Med. Chem.* **1997**, *40*, 1366.
29. Emond, P.; Guilloteau, D.; Chalon, S. *CNS Neurosci. Ther.* **2008**, *14*, 47.
30. Guilloteau, D.; Emond, P.; Baulieu, J. L.; Garreau, L.; Frangin, Y.; Pourcelot, L.; Mauclaire, L.; Besnard, J. C.; Chalon, S. *Nucl. Med. Biol.* **1998**, *25*, 331.
31. Kulkarni, S. S.; Grundt, P.; Kopajtic, T.; Katz, J. L.; Newman, A. H. *J. Med. Chem.* **2004**, *47*, 3388.
32. Yuan, H.; Petukhov, P. A. *Bioorg. Med. Chem. Lett.* **2006**, *16*, 6267.
33. Banks, R. E.; Smart, B. E.; Tatlow, J. C. *Organofluorine Chemistry: Principle and Commercial Applications*; Plenum Press: New York, 1994.
34. Filler, R.; Saha, R. *Future Med. Chem.* **2009**, *1*, 777.
35. Christensen, H. S.; Boye, S. V.; Thinggaard, J.; Sinning, S.; Wiborg, O.; Schiott, B.; Bols, M. *Bioorg. Med. Chem.* **2007**, *15*, 5262.
36. Hoffman, B. T.; Kopajtic, T.; Katz, J. L.; Newman, A. H. *J. Med. Chem.* **2000**, *43*, 4151.
37. Macdougall, I. J.; Griffith, R. *J. Mol. Graph. Model.* **2008**, *26*, 1113.
38. Paula, S.; Tabet, M. R.; Keenan, S. M.; Welsh, W. J.; Ball, W. J. J. *J. Mol. Biol.* **2003**, *325*, 515.
39. Xu, L.; Kulkarni, S. S.; Izenwasser, S.; Katz, J. L.; Kopajtic, T.; Lomenzo, S. A.; Newman, A. H.; Trudell, M. L. *J. Med. Chem.* **2004**, *47*, 1676.
40. Rogers, D.; Hopfinger, A. J. *J. Chem. Inf. Comput. Sci.* **1994**, *34*, 854.
41. Kovac, M.; Mavel, S.; Deuther-Conrad, W.; Meheux, N.; Glockner, J.; Wenzel, B.; Anderluh, M.; Brust, P.; Guilloteau, D.; Emond, P. *Bioorg. Med. Chem.* **2010**, *18*, 7659.
42. Burton, D. J. In *Organofluorine Chemistry: Techniques and Synthons*; Chambers, R. D., Ed.; Springer Verlag: Berlin Heidelberg, 1997.
43. Mikami, K.; Itoh, Y.; Yamanaka, M. *Chem. Rev.* **2004**, *104*, 1.
44. Prakash, G. K.; Yudin, A. K. *Chem. Rev.* **1997**, *97*, 757.
45. Prakesch, M.; Grée, D.; Chandrasekhar, S.; Grée, R. *Eur. J. Org. Chem.* **2005**, *2005*, 1221.
46. van Steenis, J. H.; der Gen, A. v. *J. Chem. Soc., Perkin Trans. 1* **2002**, 2117.
47. Thibonnet, J.; Duchêne, A.; Parrain, J.-L.; Abarbri, M. *J. Org. Chem.* **2004**, *69*, 4262.
48. Carcenac, Y.; Zine, K.; Kizirian, J.-C.; Thibonnet, J.; Duchêne, A.; Parrain, J.-L.; Abarbri, M. *Adv. Synth. Catal.* **2010**, *352*, 949.
49. Chenard, B. L.; Van Zyl, C. M. *J. Org. Chem.* **1986**, *51*, 3561.
50. Mitchell, T. N.; Amamria, A.; Killing, H.; Rutschow, D. *J. Organomet. Chem.* **1983**, *241*, C45.
51. Tatsuta, K.; Yamaguchi, T. *Tetrahedon Lett.* **2005**, *46*, 5017.
52. Huang, Y.; Hwang, D.-R.; Zhu, Z.; Bae, S.-A.; Guo, N.; Sudo, Y.; Kegeles, L. S.; Laruelle, M. *Nucl. Med. Biol.* **2002**, *29*, 741.
53. Chalon, S.; Hall, H.; Saba, W.; Garreau, L.; Dolle, F.; Halldin, C.; Emond, P.; Bottlaender, M.; Deloye, J. B.; Helfenbein, J.; Madelmont, J. C.; Bodard, S.; Mincheva, Z.; Besnard, J. C.; Guilloteau, D. *J. Pharmacol. Exp. Ther.* **2006**, *317*, 147.
54. Dollé, F.; Emond, P.; Mavel, S.; Demphel, S.; Hinnen, F.; Mincheva, Z.; Saba, W.; Valette, H.; Chalon, S.; Halldin, C.; Helfenbein, J.; Legaillard, J.; Madelmont, J.-C.; Deloye, J.-B.; Bottlaender, M.; Guilloteau, D. *Bioorg. Med. Chem.* **2006**, *14*, 1115.
55. Zhao, Y.; Jona, J.; Chow, D. T.; Rong, H.; Semin, D.; Xia, X.; Zanon, R.; Spancake, C.; Maliski, E. *Rapid Commun. Mass Spectrom.* **2002**, *16*, 1548.
56. Mavel, S.; Abarbri, M.; Frangin, Y.; Duchène, A.; Emond, P. *J. Pharm. Biomed. Anal.* **2004**, *35*, 193.
57. Prié, G.; Thibonnet, J.; Abarbri, M.; Duchène, A.; Parrain, J.-L. *Synlett* **1998**, *1998*, 839.
58. Qing, F.-L.; Gao, W.-Z.; Ying, J. *J. Org. Chem.* **2003**, *2000*, 65.
59. Brent, D. A.; Sabatka, J. J.; Minick, D. J.; Henry, D. W. *J. Med. Chem.* **1983**, *26*, 1014.
60. Waterhouse, R. N.; Mardon, K.; Giles, K. M.; Collier, T. L.; O'Brien, J. C. *J. Med. Chem.* **1997**, *40*, 1657.